ELectronics EXpress

LETTER

IEICE Electronics Express, Vol.13, No.12, 1–6

A controllable compact dual-band bandpass filter using loaded open-loop resonators

Ningcheng GaoDing[a)]

PRIDe Systems Engineering (or No.724) Research Institute, China Shipbuilding Industry Corporation (CSIC), Nanjing, Jiangsu 211106, People's Republic of China

a) *alex.gaoding@gmail.com*

Abstract: A compact composite open-loop resonator based dual-band band-pass filter (BPF) with high selectivity is presented. The outer open-loop and inner open-loop are corresponding to the first and second frequency passbands, respectively. The middle ring is used as the couping ring. The analysis of these open-loops has also been performed to indicate the resonance condition of the proposed filter. To demonstrate the proposed concept, the filter is fabricated with a compact size, which is 10.20 mm × 18.32 mm. The microstrip line filter is validated and measured with two passbands centered at f_1 = 3.00 GHz and f_2 = 5.34 GHz. The simulation and measured results are in good agreement.

Keywords: bandpass filter, dual-band, open-loop resonator

Classification: Microwave and millimeter-wave devices, circuits, and modules

References

[1] M. L. Chuang: "Concurrent dual band filter using single set of microstrip open-loop resonators," Electron. Lett. **41** (2005) 1013 (DOI: 10.1049/el:20051748).

[2] A. Djaiz, *et al.*: "Dual-band filter using multilayer structures and embedded resonators," Electron. Lett. **43** (2007) 527 (DOI: 10.1049/el:20070300).

[3] C. Y. Chen, *et al.*: "Design of Miniature Planar Dual-Band Filter Using Dual-Feeding Structures and Embedded Resonators," IEEE Microw. Wireless Compon. Lett. **16** (2006) 669 (DOI: 10.1109/LMWC.2006.885621).

[4] M. Hayati, *et al.*: "Compact dual-band bandpass filter using open loop resonator for multi-mode WLANs," Electron. Lett. **48** (2012) 573 (DOI: 10.1049/el.2012.0439).

[5] X. Luo, *et al.*: "Compact Dual-Band Bandpass Filters Using Novel Embedded Spiral Resonator (ESR)," IEEE Microw. Wireless Compon. Lett. **20** (2010) 435 (DOI: 10.1109/LMWC.2010.2050195).

[6] S. Yang, *et al.*: "Design of compact dual-band bandpass filter using dual-mode stepped-impedance stub resonators," Electron. Lett. **50** (2014) 611 (DOI: 10.1049/el.2013.4217).

[7] H. J. Yuan and Y. Fan: "Compact microstrip dual-band filter with stepped-impedance resonators," Electron. Lett. **47** (2011) 1328 (DOI: 10.1049/el.2011.2671).

[8] L. Ren and H. Huang: "Dual-band bandpass filter based on dual-plane

DOI: 10.1587/elex.13.20160470
Received May 10, 2016
Accepted May 18, 2016
Publicized June 3, 2016
Copyedited June 25, 2016

microstrip/interdigital DGS slot structure," Electron. Lett. **45** (2009) 1077 (DOI: 10.1049/el.2009.1851).
[9] X. Jin, *et al.*: "Compact dual-band bandpass filter using single meander multimode DGS resonator," Electron. Lett. **49** (2013) 1083 (DOI: 10.1049/el.2013.0977).
[10] J. Shi, *et al.*: "A Quasi-Elliptic Function Dual-Band Bandpass Filter Stacking Spiral-Shaped CPW Defected Ground Structure and Back-Side Coupled Strip Lines," IEEE Microw. Wireless Compon. Lett. **17** (2007) 430 (DOI: 10.1109/LMWC.2007.897791).
[11] H. W. Liu, *et al.*: "Compact dual-band bandpass filter using defected microstrip structure for GPS and WLAN applications," Electron. Lett. **46** (2010) 1444 (DOI: 10.1049/el.2010.2146).
[12] Z.-C. Zhang, *et al.*: "Compact Dual-Band Bandpass Filters Using Open-/Short-Circuited Stub-Loaded $\lambda/4$ Resonators," IEEE Microw. Wireless Compon. Lett. **25** (2015) 657 (DOI: 10.1109/LMWC.2015.2463216).
[13] S. Zhang and L. Zhu: "Compact Split-Type Dual-Band Bandpass Filter Based on $\lambda/4$ Resonators," IEEE Microw. Wireless Compon. Lett. **23** (2013) 344 (DOI: 10.1109/LMWC.2013.2264659).
[14] X. Y. Zhang, *et al.*: "Dual-Band Bandpass Filters Using Stub-Loaded Resonators," IEEE Microw. Wireless Compon. Lett. **17** (2007) 583 (DOI: 10.1109/LMWC.2007.901768).
[15] R. H. Geschke, *et al.*: "Filter Parameter Extraction for Triple-Band Composite Split-Ring Resonators and Filters," IEEE Trans. Microw. Theory Techn. **59** (2011) 1500 (DOI: 10.1109/TMTT.2011.2123109).

1 Introduction

In recent, multi-band and multi-function wireless systems have been gaining much attention. It is important to keep these systems to a minimum size and high selectivity. Therefore, the systems prefer multiband transceiver to multiple single band ones. To response this need, multi-band BPFs are intensively investigated and various design approaches have been reported [1, 2, 3, 4, 5, 6, 7]. The dual-band BPF can be realized by utilizing planar filter with open-loop resonator [1]. However, the open-loop dual-band BPFs normally occupy larger circuit size due to the parallel or cascaded structures. In order to reduce the size, stepped-impedance resonators (SIRs) with multi-layer structure has been reported in [2] with controlling lower and upper passbands. To fabricate the dual band open-loop resonators in a single layer, multiple open-loop resonators have been embedded at the ends of the first passband open-loop resonator [3, 4, 5]. However, the vias made the open-loop resonator design more complex. Nevertheless, this sort of dual band BPFs need a large number of resonators to generate two passbands. Some other techniques have also been reported to realize the dual-band BPFs. In [6, 7], stepped impedance resonators have been applied to enhance the selectivity of the filters. The defected ground structure (DGS) [8, 9, 10] and defected microstirp structure (DMS) [11] have been also reported. Meanwhile, the dual-band using the quarter-wavelength resonator as the loaded stub and the split resonator has been analyzed in [12, 13]. Hence, key issues of the dual-band BPFs can be summarized as independent control of the passband frequency, high selectivity, and compact size.

DOI: 10.1587/elex.13.20160470
Received May 10, 2016
Accepted May 18, 2016
Publicized June 3, 2016
Copyedited June 25, 2016

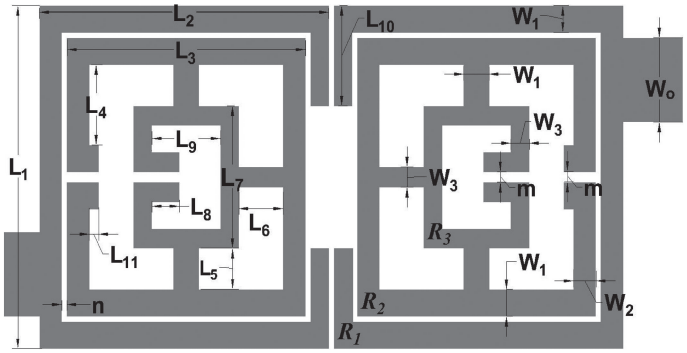

Fig. 1. Schematic of the proposed dual-band filter

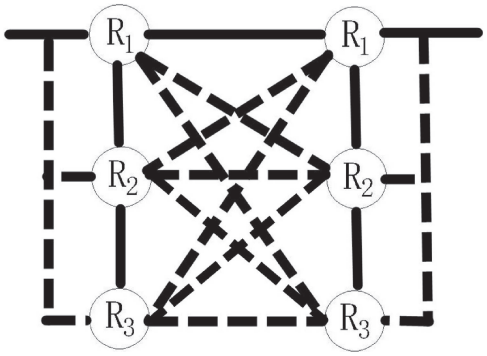

Fig. 2. The coupling schematic of the proposed dual-band filter

A compact dual-band filter using three sets of open-loop resonators with loaded structure is introduced to solve the above problems. The proposed filter can generate four transmission zeros (TZs) which improve the selectivity. The first and the second passband frequencies, namely f_1 and f_2, can be controlled independently and the bandwidth of the second passband frequency can also be tunable. The three sets of rings embedded with each other. The outer and inner rings are corresponding to the f_1 and f_2. The middle ring is used as the coupling ring between the first and the third rings. It increases the design freedom of the second passband frequency which overcomes the large gap between two rings caused by the large frequency space between them. Open-loop resonators and the proposed structure conditions are analyzed and demonstrated. A prototype filter is fabricated with compact size and the measured result is presented.

2 Analysis of the proposed dual-band filter

The schematic of proposed dual-band filter with open-loop resonators is shown in Fig. 1. Three open-loop resonators located from outer to inner, namely R_1, R_2 and R_3. R_1 and R_3 are corresponding to the f_1 and f_2, respectively. As the analysis in [14], the electrical lengths of these two resonators should be equal to the half guided wavelength to the corresponding passband frequency f_1 and f_2 to satisfy the resonance condition. There are six rings in this design which are a pair of R_1, R_2 and R_3. This coupling structure can be modeled by the full coupling model [15]. The coupling schematic has been shown in Fig. 2. In this schematic, the solid lines represent the major coupling and the dash lines represent the cross coupling. The

DOI: 10.1587/elex.13.20160470
Received May 10, 2016
Accepted May 18, 2016
Publicized June 3, 2016
Copyedited June 25, 2016

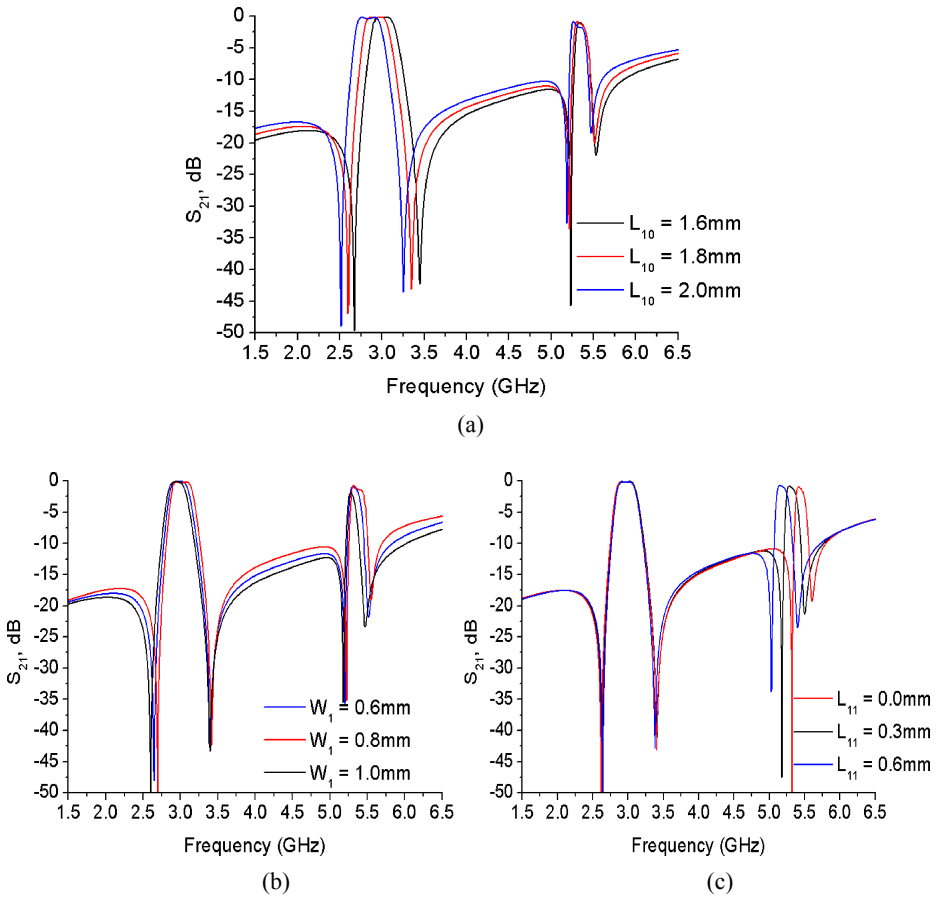

Fig. 3. (a) Simulated results of the tunable f_1 (b) Simulated results of the f_2 bandwidth tuning (c) Simulated results of the tunable f_2

cross couplings between the inner resonators and source or load are very small [15]. As the topology shown in Fig. 2, R_1 is the major coupling path for f_1 and f_2 from the input to output and R_2 is used as a coupling ring. With this structure, the end coupling and multi-path of R_1, R_2 and R_3 help generate the TZs for the proposed filter [14, 15]. Since the gaps, n and m as shown in Fig. 1, also play an important role in the coupling coefficients, bandwidth and TZs positions [14, 15], there is a compromise between them to realize the filter specifications. To verify the coupling structure, the electromagnetic simulator has been used to simulate the proposed filter and to illustrate the specific stubs and gaps performance on the proposed filter. Firstly, once R_1 decided, the first passband frequency is set up. Through tuning the length from the end of R_1, the f_1 can be shifted with slight influence on the other two frequencies. The simulated result is shown in Fig. 3(a). The slightly insert loss increasing of f_2 is due to the length changes of L_{10} as shown in Fig. 1, which made a contribution to the coupling coefficient of f_2. Due to the relative large frequency space between f_1 and f_2, the ring sizes between R_1 and R_3 are also distinctive. The coupling through the certain gap may lead to weak coupling unless the change of the size of R_3 or loaded the R_3 onto the R_1 [3, 4]. However, this will also change the third passband frequency response or ascend the size of the proposed filter. To solve this, R_2 is also used as a coupled ring between R_3 and R_1 to create the path for f_2. The mainly coupling part is L_2 and L_3 as shown in Fig. 1. The three stubs are

DOI: 10.1587/elex.13.20160470
Received May 10, 2016
Accepted May 18, 2016
Publicized June 3, 2016
Copyedited June 25, 2016

located centrally between the R_2 and R_3 which are used to enhance the coupling between R_2 and R_3 instead of the utility of the gap coupling [2]. Each stub is located centrally between R_2 and R_3 and in parallel with them. Therefore, the admittances of the three stubs have moderate influence on the performances of the passband frequencies and their bandwidths. Furthermore, it also indicates that, through tuning the width of the L_2 in Fig. 1, the bandwidth of f_2 can be tuned due to the coupling condition changes between R_1 and R_2. The simulated results are shown in Fig. 3(b). The coupling condition is such that the L_{11} has also made a significant contribution to the coupling coefficient for the f_2. Hence, f_2 can be tuned through changing the parameter of R_2 without altering f_1 and the size of R_3. The simulated results illustrated in Fig. 3(c). As a summary, f_1 is 3 GHz, 2.85 GHz and 2.7 GHz at $L_{10} = 1.6$ mm, 1.8 mm and 2.0 mm respectively. Meanwhile, f_2 is 5.15 GHz, 5.34 GHz and 5.52 GHz at $L_{11} = 1.6$ mm, 1.8 mm and 2.0 mm respectively.

3 Experimental results and comparisons

In this design, HFSS 12 has been used as the electromagnetic simulator to realize the resonant frequency responses. The substrate of the filter has relative dielectric constant of 2.65 and thickness of 0.93 mm. The dimensions of the filter regarding the Fig. 1 are as follows (all in mm): $W_o = 2.49$, $W_1 = 0.8$, $W_2 = 0.7$, $W_3 = 0.6$, $L_1 = 10.20$, $L_2 = 9.08$, $L_3 = 7.49$, $L_4 = 2.38$, $L_5 = 1.22$, $L_6 = 1.39$, $L_7 = 4.23$, $L_8 = 0.7$, $L_9 = 2.15$, $L_{10} = 2.6$, $L_{11} = 0.3$, $m = 0.3$, $n = 0.16$, which is $0.15\lambda_g \times 0.26\lambda_g$ as shown in Fig. 4. The λ_g here is the guided wavelength of the first passband frequency and the W_o is the characteristics impedance of 50 Ω. An Agilent N5230C vector network analyzer (VNA) is used to measure the frequency response of the proposed filter. As shown in Fig. 5, measured and simulated results from 1.5 to 6.5 GHz have been compared and shown a good agreement. The center frequencies of the two pass bands are 3.00 GHz and 5.34 GHz with 3 dB fractional bandwidths (FBWs) of 10% and 3.7%, respectively. The four TZs are located at 2.65 GHz, 3.50 GHz, 5.23 GHz and 5.56 GHz. The insert losses of the corresponding pass bands are 0.19 dB and 2.34 dB. The slightly frequency drifting is due to the manufacture errors. In the Table I, the dual-band BPF here has been used to compare with other relative works. From the comparison, it illustrated that, through a simply open-loop resonator structure, the proposed filter realized a compact size and relative large frequency space between f_1 and f_2.

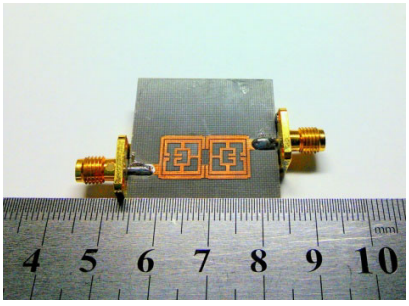

Fig. 4. Photograph of fabricated dual-band filter

DOI: 10.1587/elex.13.20160470
Received May 10, 2016
Accepted May 18, 2016
Publicized June 3, 2016
Copyedited June 25, 2016

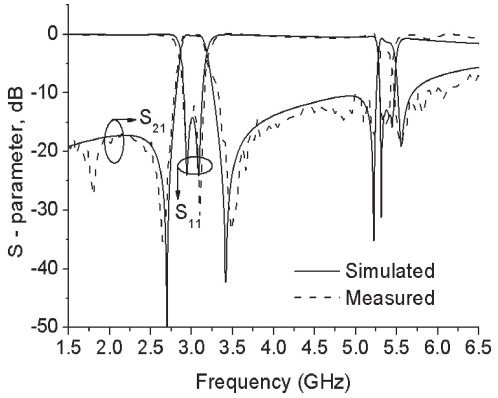

Fig. 5. Measured and simulated results of the proposed dual-band filter

Table I. Comparison with some relative dual-band BPFs

References	Techniques	Frequencies (GHz)	3 dB FBWs (%)	Size ($\lambda_g \times \lambda_g$)
1	Open-loop	1.00, 2.20	5/5.2	0.60×1.80
2	Multi-layer	2.45, 5.80	N/A	0.11×0.21
6	SISR	1.84, 2.65	N/A	0.17×0.21
8	DMS	1.57, 2.40	10/3.7	0.27×0.40
13	$\lambda/4$ resonator	1.73, 2.45	5, 5	0.14×0.345
This work	Open-loop	3.00, 5.34	10, 3.7	0.15×0.26

4 Conclusion

A compact dual-band bandpass filter with four transmission zeros using loaded open-loop resonator is presented. The analysis of the three set resonators has been illustrated and the results have been showed. The three stubs and the coupling ring structure are used to improve the performance. Through these improvements, the proposed filter realized a very compact size and the good tunable performance. The filter has also been fabricated and validated the proposed concept. The simulated and measured results are in good agreement.

Acknowledgments

This work was supported by the National Key Scientific Instruments and Equipment Development Project under Grant No. 2013YQ290451.

DOI: 10.1587/elex.13.20160470
Received May 10, 2016
Accepted May 18, 2016
Publicized June 3, 2016
Copyedited June 25, 2016